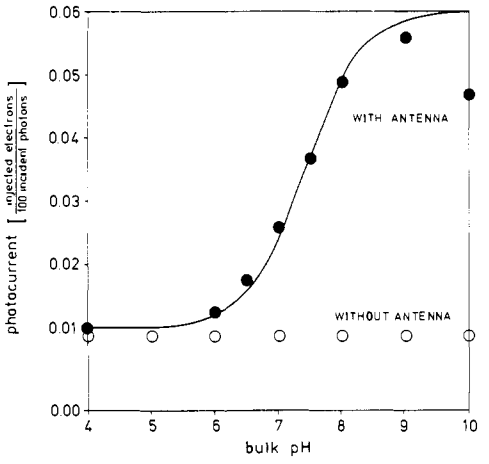

Figure 10. Sensitized photocurrent of complete antenna assembly with illumination of antenna pigment (380 nm) under constant-field condition in the space charge as a function of pH. The data are fitted by an ideal titration curve with a pK taken from fluorescence titration of the antenna (Figure 6). The circles indicate the background in a system without antenna.

However, in that potential range the intrinsic photocurrent is strongly pH dependent, as shown in Figure 7b for a wavelength of 330 nm. At the wavelength of antenna excitation, 380 nm, this current is lower (Figure 8), but still of the same order as the antenna-sensitized current.

The interference of antenna and background could be bypassed by a pigment system with energies far from the band edge. However, an antenna dye which matches all the other requirements of the device (pK near neutrality, steep titration curve, high quantum yield of fluorescence, and high absorbance at the longer wavelength) is not available at the present moment.

The background current may be suppressed by applying a lower electrode potential (Figure 7b). In that potential range, however, a strong pH dependence of the electron injection current appears (Figure 7c), which is due to the changing yield of charge removal as modulated by the pH-dependent Helmholtz layer (eq 20). In order to titrate the device with constant yield q_{rel}, the field in the space charge has to be held pH invariant.

This constant-field condition is realized by following the pH change of the Helmholtz potential with the external potential, such that the bands are held at constant slope (Figure 2). Since the Helmholtz potential changes constantly by about −59 mV per pH unit, this procedure may be realized without fit during the titration. Figure 9 shows the result of a constant-field titration near the half-wave potential of the injection current. The circles refer to the saturation current 480 mV about the flatband potential, observed at 470 nm with the complete assembly. The dots show the half-wave current 120 mV above V_{FB}. Perfect compensation of the pH influence is achieved. On top of Figure 9 the standard potential/pH line of −60 mV per pH unit used for compensation is compared to the measured flatband and half-wave potentials. Such a standard line is used since the actual slope varies somewhat from batch to batch.

Under these constant-field conditions the photocurrent with excitation of the antenna at 380 nm is shown in Figure 10 as a function of pH. The data are fitted according to eq 23–25 by an ideal titration curve for i_{CM} with pK = 7.4 as taken from antenna fluorescence of Figure 6 and a constant background i_{SC}. Perfect agreement of fluorescence and photocurrent titration is apparent.

This is the realization of sequential energy–electron transfer modulated by protons. The switching experiment shown in Figure 3 is made under identical conditions. The chemical nature of the coumarin pigment is imprinted onto the electrical response of the semiconductor by sequential energy and electron transfer.

An Empirical Valence Bond Approach for Comparing Reactions in Solutions and in Enzymes

Arieh Warshel* and Robert M. Weiss

Contribution from the Department of Chemistry, University of Southern California, Los Angeles, California 90007. *Received March 3, 1980*

Abstract: A simple and reliable empirical valence bond (EVB) approach for comparing potential surfaces of reaction in solution and in enzymes is developed. The method uses the valence bond concept of ionic–covalent resonance to obtain a Hamiltonian for the isolated molecule and then evaluates the Hamiltonian for the reaction in solution by adding the calculated solvation energies to the diagonal matrix elements of the ionic resonance forms. The resulting potential surface is then calibrated by using pK_a measurements and other information about the reaction in solution. The calibrated potential surface provides a simple tool for comparing the activation energy of a reaction in solution with that in an enzyme by replacing the solvation energies of the ionic resonance forms by their interactions with the enzyme active site. The EVB method is illustrated by calculations of typical solution reactions including an ionic bond-breaking reaction, a proton-transfer reaction, and a general-acid catalysis reaction. The application of the EVB method to studies of enzymic reactions is demonstrated by calculating the potential surface for the rate-limiting step of the catalytic reaction of lysozyme and comparing the calculated activation energy to that of the reaction in solution.

I. Introduction

It is known that the environment in which a reaction occurs can influence the reaction rate profoundly. Large rate enhancements have been observed upon increasing solvent polarity (see for example, ref 1). This is particularly true for a large class of bond-breaking and -forming reactions that pass through ionic or partially ionic transition states. Thus, it is important to develop a theoretical method able to compare potential surfaces of these reactions as the environment is changed.

Early in the development of quantum chemistry considerable progress was made with the valence bond picture of chemical bonding, but the approach was largely abandoned during the last 30 years for molecular orbital methods. These methods (which are much simpler than valence bond to implement in ab initio approaches) have had considerable success in many areas but have

(1) Wiberg, K. B. "Physical Organic Chemistry"; Wiley: New York, 1963.

0002-7863/80/1502-6218$01.00/0

not provided a practical and reliable calculation scheme for treating environmental effects on chemical reactions. It seems to us that for this type of problem the right strategy is to use the valence bond approach, which treats the existence of ionic and covalent resonance forms in a way closely related to chemical intuition. This makes empirical evaluation of the isolated molecule Hamiltonian quite simple.[2,5-9] More importantly, the most significant contribution of the environment appears as electrostatic effects that change enormously with the ionic character of the reacting system. These effects can be introduced explicitly and consistently into the valence bond Hamiltonian by including the electrostatic stabilization of the ionic resonance forms in their diagonal matrix elements.

In this paper, we describe the extension of the valence bond approach to empirical evaluation of the effects of different environments on chemical reactions, in particular comparison of aqueous solutions with enzyme active sites.

In section II, we outline our approach, showing how to evaluate the isolated molecule Hamiltonian and how to evaluate and calibrate the solution Hamiltonian. Section III demonstrates the use of our approach in constructing the potential surface for proton-transfer and general-acid catalysis reactions and more importantly, in evaluating the energetics of enzyme catalysis by *quantitative* comparison of the potential surface for general-acid catalysis of sugar hydrolysis in solution and in the active site of lysozyme.

II. Methods

1. Overview. We describe here an empirical valence bond (EVB) technique of comparing quantitatively the effects of different environments on reaction potential surfaces. The basic task of the method involves construction of a secular equation whose elements, functions of reactant geometry, reflect the energies and interactions of resonance forms which contribute to the properties of reactants, intermediates, or products. Solution of the secular equation gives the energy of the reaction system in the assumed geometry.

The EVB method represents the reacting system as a superposition of ionic and covalent resonance forms. In this representation, the major effect of changing the reaction environment is to alter the electrostatic interaction of the ionic resonance forms with the surroundings. This can be realized, for example, by considering the energy involved in separating two ionized atoms. In the gas phase, this energy could be approximated by eq 1, where

$$E^g(r) = -e^2/r + V_{nb}(r) \tag{1}$$

V_{nb} represents a nonbonded interaction significant only at small separations. The comparable energy in solution is

$$E^s(r) = -e^2/r + V_{nb}(r) + G_{sol}{}^s(r) \tag{2}$$

where G_{sol} is the solvation free energy of the two ions and can be on the order of 70 kcal/mol for two ions 3 Å apart in a high-dielectric medium. In the active site of an enzyme

$$E^{enz}(r) = -e^2/r + V_{nb}(r) + G_{sol}{}^{enz}(r) \tag{3}$$

where $G_{sol}{}^{enz}$ is the interaction between the ions and the enzyme charges and induced dipoles.[10] This energy can also be on the order of 70 kcal/mol for an ion pair at a 3-Å separation. On the other hand, the energy of the covalent forms is not expected to be changed so much by the solvent or the enzyme. The consequent large change in the relative energies of the ionic and covalent resonance forms leads to a drastic change in their mixing and to change in the energy and ionic character of the ground electronic state. The EVB approach is based on the assumption that the most important environmental effect is the above change in the relative energies of the ionic and covalent states.

The method incorporates this effect in a practical calculation scheme that is outlined in the next three sections: The first section describes the EVB formalism. The second section outlines the evaluation of the solvation energy and its introduction in the EVB Hamiltonian. The third section outlines the use of the EVB Hamiltonian in comparing enzyme and solution reactions.

2. Constructing the EVB Hamiltonian for Solution Reactions. The user of the EVB method must choose, on the basis of experience and intuition, a set of bonding arrangements or "resonance forms" which can describe the reacting system throughout the course of the reaction. Each can involve covalent, ionic, or a mixture of bonding types closely related to bonding diagrams frequently used in organic chemistry text books.

We use below (section a) the ionic bond cleavage reaction

$$X\text{–}Y \rightarrow X^- + Y^+ \tag{4}$$

as an example; the construction of the EVB Hamiltonian for more complicated reactions is discussed in section b.

(a) EVB Hamiltonian for Ionic Bond Cleavage. The ionic bond cleavage of eq 4 can be described by the three resonance forms in eq 5, where ψ_i denotes both the resonance form and its wave

$$\psi_1 = X\text{–}Y \qquad \psi_2 = X^-Y^+ \qquad \psi_3 = X^+Y^- \tag{5}$$

function. If X is more electronegative than Y, then the most important resonance forms are ψ_1 and ψ_2. Note that ψ_1 describes a purely covalent bond and not the real bond, which includes some component of ψ_2.

The potential energy surfaces for the isolated molecule result from mixing of these resonance forms and are given by the solutions E^g of the secular equation (6), where $H_{ij}{}^g = \int \psi_i H^g \psi_j$ is

$$\begin{vmatrix} H_{11}{}^g - E^g & H_{12}{}^g - E^g S_{12} \\ H_{21}{}^g - E^g S_{21} & H_{22}{}^g - E^g \end{vmatrix} = 0 \tag{6}$$

the Hamiltonian matrix element for the isolated (gas-phase) molecule. We neglect the overlap matrix elements $S_{ij} = \int \psi_i \psi_j$, although the method does not require this. We expect some of the errors so introduced to be compensated by the empirical calibration of the off-diagonal Hamiltonian elements (see below). Several methods can be used to obtain the H_{ij} as functions of the reactant geometry. The matrix elements can be calculated ab initio from the atomic orbital wave functions involved or semiempirically. Here we follow mainly the empirical procedure of Coulson and Daniellson[5] to obtain matrix elements closely related to experiment.

The diagonal matrix elements of the Hamiltonian have clear physical meaning. They are the energies of the related resonance forms. An empirical function incorporating bond stretching, electrostatic and steric nonbonded interactions as well as other terms can be constructed for each resonance form. In our example of bond cleavage, we follow ref 5 and approximate the diagonal element of the covalent resonance form by a Morse-type potential function (7), where r is the X–Y bond length, the parameter r_0

$$E_1{}^g = H_{11}{}^g = \bar{M} \tag{7}$$

$$\bar{M} = \bar{D}\{\exp[-2a(r - r_0)] - 2\exp[-a(r - r_0)]\}$$

is taken as the gas-phase equilibrium bond length of the X–Y bond, and a is determined from the stretching vibrational frequency. The parameter $\bar{D}$ is approximated by the geometric mean formula (eq 8) which is meant to describe the dissociation energy of a purely covalent resonance form.[2,5]

$$\bar{D} = (D_{XX}D_{YY})^{1/2} \tag{8}$$

(2) Pauling, L. "The Nature of the Chemical Bond"; Cornell University Press: Ithaca, NY, 1960.
(3) Eyring, H.; Walter, J.; Kimball, G. E. In "Quantum Chemistry;" Wiley: New York, 1944; Chapter 13.
(4) Craig, D. P. *Proc. R. Soc. London, Ser. A*, **1950**, *200*, 390–409.
(5) Coulson, C. A.; Danielsson, U. *Ark. Fys.* **1954**, *8*, 239–255.
(6) Warhurst, E. *Trans. Faraday Soc.* **1949**, *45*, 461–476.
(7) Baughan, E. C.; Evans, M. G.; Polanyi, M. *Trans. Faraday Soc.* **1941**, *37*, 377–393.
(8) Warhurst, E. *Proc. R. Soc. London, Ser. A* **1951**, *207*, 32–49.
(9) Warshel, A.; Bromberg, A. *J. Chem Phys.* **1970**, *52*, 1262–1269.
(10) Warshel, A. *Proc. Natl. Acad. Sci. U.S.A.* **1978**, *75*, 5250–5254.

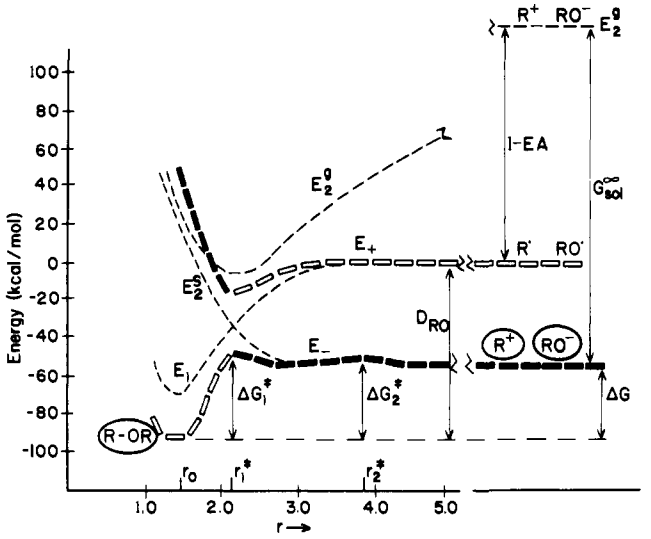

Figure 1. Ionic bond cleavage in solution. The result of calculations for the reaction R–O–R′ → $R^+ + R'O^-$, where R and R′ are sugar residues. E_1, E_2^g and E_2^s are respectively the energies of the covalent, gaseous ionic, and aqueous ionic resonance forms. E_- and E_+ are the ground- and excited-state energies in solution, ΔG is the reaction free energy, $\Delta G_2^* - \Delta G$ is the barrier for forming the ion pair in the solvent cage, and ΔG_1^* is the activation barrier at r_1^*, where E_1 and E_2^s intersect. The regions of the surfaces that correspond to an ionic state are shown as ▬ ▬ and those that correspond to a covalent state as ▭ ▭.

The second resonance form corresponds to an ionic state; its energy is approximated by eq 9, where $\Delta^{(2)}$ is the gas-phase

$$E_2^g = H_{22}^g = \Delta^{(2)} - e^2/r + V_{nb}^{(2)} \quad (9)$$

formation energy of X^-Y^+ from X·Y· at infinite separation ($\Delta^{(2)} = I_Y - EA_X$), EA and I are electron affinity and ionization potential, and V_{nb} is a nonbonded potential function chosen so that the minimum of $(-e^2/r + V_{nb})$ is given by the sums of the ionic radii of X^- and Y^+.

The off-diagonal element H_{12}^g is determined, following ref 5, by using the fact that the eigenvalues of the Hamiltonian, E, satisfy the relation $H_{12}^2 = (H_{11} - E)(H_{22} - E)$ on neglect of overlap. We take E as the experimental ground-state bond energy. This gives

$$H_{12}^g = [(E_1^g - M_{XY})(E_2^g - M_{XY})]^{1/2} \quad (10)$$

where M_{XY} is a Morse potential for the real X–Y bond that reproduces the observed dissociation energy, D_{XY}, equilibrium bond length r_0, and stretching frequency. Equation 10 can be expressed in the form:

$$H_{12}^g = L_{12}(r_{XY}) \quad (11)$$

Having the gas-phase empirical Hamiltonian, we approximate the solution Hamiltonian, H^s, by leaving the covalent and off-diagonal terms unchanged ($H_{11}^s = H_{11}^g$; $H_{12}^s = H_{12}^g$) and changing only the diagonal matrix elements of the ionic resonance forms by adding in the appropriate solution free energy:

$$E_2^s = H_{22}^s = E_2^g + G_{sol}^{(2)} \quad (12)$$

where $G_{sol}^{(2)}$ is the solvation free energy of the X^-Y^+ ion pair, evaluated with the use of the ground-state orientation of the permanent dipoles of the solvent (see section 3). In the calculation of an enzymic reaction $G_{sol}^{(2)}$ is the electrostatic interaction between the ion pair and the rest of the enzyme–substrate complex.

The ground- and excited-state energy surfaces for the bond cleavage reaction are obtained now by diagonalizing the solution Hamiltonian and are given by:

$$E_\pm = \tfrac{1}{2}[(E_1^s + E_2^s) \pm ((E_1^s - E_2^s)^2 - 4(H_{12}^s)^2)^{1/2}] \quad (13)$$

As an example of evaluation of potential surfaces for bond-breaking reactions, we present in Figure 1 calculations of E_- and E_+ for heterolytic cleavage of the glycosidic bond of a disaccharide. The figure demonstrates how the very large contribution of G_{sol} makes the ionic resonance form the ground state for $r > r_1^*$. The potential surface for this solvated ionic ground state is nearly a horizontal line with two low-energy activation barriers, one at r_2^*, where the ions are combined in the same solvent cage, and the second at r_1^*, where E_1 and E_2 intersect. This result persists in preliminary calculations of other ionic bond cleavage reactions, predicting diffusion-controlled rates for ion recombination in agreement with the measurements of Eigen and de Maeyer.[11]

(b) EVB Matrix Elements for More Complicated Systems. The generalization of the EVB Hamiltonian to more complicated reactions is straightforward. It requires evaluation of four types of matrix elements: (i) Diagonal matrix elements of the covalent states, which are assumed to be equal in solution and the gas phase and are approximated by potential functions of the form (14),

$$E_{(i)}^{cov} = \sum_k \bar{M}_k(r_k) + V_{nb}^{(i)}(\mathbf{r}) \quad (14)$$

where the $\bar{M}_k$ is a Morse potential function for the kth bond and $V_{nb}^{(i)}$ is the sum of the nonbonded interactions in the ith resonance form between atoms not bonded to a common atom. (ii) Diagonal matrix elements of the ionic states, which are taken as the sum of an isolated molecule energy and a solvation energy and are approximated by potential functions of the form (15), where $\Delta^{(j)}$

$$E_{(j)}^{ion} = \Delta^{(j)} + V_{QQ}^{(j)} + V_{nb}^{(j)} + G_{sol}^{(j)} \quad (15)$$

is the isolated molecule energy of forming the charged fragments in the jth configuration at infinite separation, $V_{QQ}^{(j)}$ is the electrostatic interaction between the charged fragments in the ith configuration, $V_{nb}^{(j)}$ is the nonbonded interaction between the fragments (exluding $V_{QQ}^{(j)}$) and $G_{sol}^{(j)}$ is the solvation free energy of the jth configuration (see Section 3). (iii) Off-diagonal elements H_{ij} that couple configurations which differ by the presence of one bond, l, are given by eq 16, where $L_{ij}(r_l)$ is L_{ij} of eq 11 evaluated

$$H_{ij} = L_{ij}(r_l) \quad (16)$$

at r_l with all uninvolved fragments held at infinity. In this way, these matrix elements are calibrated by the requirement that the dependence of E_i^g on r_l with all other r fixed at infinity reproduce the gas-phase Morse potential for the lth bond. (iv) Off-diagonal elements H_{ij} that couple configurations that differ by the presence of more than one bond are set to zero (following ref 4) since they are proportional to the square (or higher powers) of the overlap between the corresponding atomic orbitals (in some cases, however, we may follow ref 5 and retain these terms by using the proper analytical expression). When all the fourth type of matrix elements are set to zero, the entire Hamiltonian is closely related to experimentally determined quantities. Having obtained all the matrix elements of H, we obtain the ground-state energy as the lowest eigenvalue of the secular equation

$$\mathbf{H}\mathbf{c}_i = E_i\mathbf{c}_i \quad (17)$$

3. Calculation of Solvation Energies in Solution and Inside Proteins. Comparison of solution and enzymic reactions requires evaluation of the solvation energies $G_{sol}^{(i)}$ of the ionic resonance forms in polar solvents and in protein active sites. The solvent is treated by the previously developed microscopic models.[12,13] Here, we outline the main features of these models and describe the modifications needed for treating interactions of the charge distribution of the ionic resonance forms with the permanent and induced dipoles of the solvent.

(a) Solvation of Ionic Resonance Forms in Aqueous Solutions. In previous works, we estimated the solvation energy of charged systems in aqueous solution by the surface constrained soft sphere dipoles (SCSSD) approach,[13] which represents the water molecules as point dipoles attached to the centers of soft spheres and minimizes the solute–solvent and solvent–solvent energies with respect to the orientation and position of these dipoles. The solvation energy is then given by the difference between the minimum

(11) Eigen, M.; de Maeyer, L. In "Technique of Organic Chemistry", 2nd ed., A. Weissberger, Ed., Interscience: New York, 1963.
(12) Warshel, A.; Levitt, M. *J. Mol. Biol.* **1976**, *103*, 227–249.
(13) Warshel, A. *J. Phys. Chem.* **1979**, *83*, 1640–1652.

energy of the solute–solvent system and the energy of the solvent. Because the calculations are limited to a few solvation shells, these are surrounded by a surface of dipoles in the positions of the bulk solvent. The model was calibrated to reproduce solvation enthalpies of ions at 300 K.

We must adapt the SCSSD model to the EVB method in order to be consistent with the Born–Oppenheimer approximation; for a given reactant geometry the solvent nuclei must be fixed while the solvation energies of all the resonance forms involved are calculated. This is accomplished here by replacing the permanent dipoles of the SCSSD model by a combination of permanent and induced dipoles, fixing the permanent dipoles in orientations that minimize the energy of the ground electronic state and allowing the induced dipoles to be polarized differently for each electronic resonance form. This is consistent with both intuition and the Born–Oppenheimer approximation, since the positions and orientations of the permanent dipoles (which represent the solvent nuclear coordinates) cannot simultaneously have several values, while the orientations and magnitude of the induced dipoles represent the solvent electronic distribution, which is different for different electronic wave functions of the solute–solvent system. The practical implementation of this approximation in the evaluation of the $G_{sol}^{(i)}$ involves the following steps: (i) The solvent SCSSD model is modified, replacing the permanent dipoles by a combination of permanent and induced dipoles:

$$\mu_j = 0.65\mu_{SCSSD} + \alpha \mathbf{E}_j \tag{18}$$

where $|\mu_{SCSSD}|$ is the magnitude of the original SCSSD permanent dipole, α is the polarizability of a water molecule (taken as 1.2 Å^3), and $\mathbf{E}_j$ is the field at the jth solvent molecule produced by the solute charges and the other solvent molecules. (ii) The orientations and positions of the solvent permanent dipoles are determined by using the ground-state charge distribution of the solute molecule and energy minimization as described above. (iii) $G_{sol}^{(i)}$ for the ionic configurations are determined by fixing the permanent solvent dipoles in their ground-state configuration and minimizing the energy of the solute–solvent system by iterative evaluation of the induced dipoles $\alpha\mathbf{E}$ with use of the field from the assumed charges of the solute in its ith configuration and from the solvent dipoles. (iv) A new ground-state charge distribution is evaluated for the solute molecule by using the above $G_{sol}^{(i)}$ and solving eq 17. Steps ii, iii, and iv are repeated until convergence is achieved. The SCSSD model in this form is calibrated to give ionic free energies of solvation at 300 K; these are about 5% smaller than solvation enthalpies at 300 K.[13]

(b) Stabilization of Ionic Resonance Forms in Proteins. The stabilization ("solvation") energies, $G_{sol}^{(i)}$, of the ionic resonance forms in enzyme active sites are calculated by evaluating the interaction between the charges of these resonance forms and the partial charges and induced dipoles of the enzyme atoms. Since the enzyme atoms remain fixed in their X-ray determined positions, this procedure is consistent with the Born–Oppenheimer approximation. The solvation energy is made up of the following contributions: (i) The charge–charge interactions, which are given (in kcal/mol for r in Å) by eq 19, where j runs over reacting and

$$V_{Qq}^{(i)} = 332\sum_{jj'} Q_j^{(i)} q_{j'}/r_{jj'} \tag{19}$$

j' over protein atoms, $r_{jj'}$ is the distance between the j and j' atoms, the q are the point charges of the protein, and the $Q^{(i)}$ are the charges of the substrate in the ith resonance form. (ii) The inductive interactions between the charges of the substrate and the polarizable electrons of the protein atoms. These contributions are evaluated by assigning induced dipoles, μ_k, to all the protein atoms and calculating self-consistently the magnitudes and directions of these dipoles in the presence of the substrate and protein charges and each other. The interaction of the induced dipoles with the substrate and protein charges is given (in kcal/mol for r in Å) by eq 20. The details of this procedure and useful simplifications are given in ref 12.

$$V_{Q\alpha}^{(i)} = -166\sum Q_j^{(i)}\mu_k \mathbf{r}_{jk}/r_{jk}^3 - 166\sum_{j',k} q_{j'}\mu_k \mathbf{r}_{j'k}/r_{j'k}^3 \tag{20}$$

(4) Empirical Calibration of the Solution Hamiltonian for Comparison with Enzymic Reactions. The potential surface obtained in previous sections offers a convenient model for a *qualitative* estimate of the ionic character of transition states in solution and of solvent effects on ground states of polar molecules. This is, however, not the primary aim of the present work, which is mainly concerned with *quantitative comparison* of potential surfaces in aqueous solution with those in enzyme active sites. In order to improve the quality of the results, we calibrate the solution Hamiltonian by forcing the calculated ground-state energy at certain points to reproduce their experimentally determined free energies. For example, in the case of the ionic bond cleavage discussed above, the calibration involves adjusting $\Delta^{(2)}$ by fitting the calculated energy change to reproduce the observed ΔG of reaction in solution with the use of relation (21). Similarly, in

$$E_-(\infty) - E_-(r_0) = \Delta G_{obsd} \tag{21}$$

the case of proton-transfer reactions AH + B → A$^-$ + BH$^+$ (discussed in section III) the calibration involves adjustment of the Δ parameter of the A$^-$ BH$^+$ resonance form to fit calculated and observed free energies of proton transfer. In some cases, it is useful to calibrate the off-diagonal matrix element by constraining $\Delta G^{\ddagger}_{calcd}$ to reproduce $\Delta G^{\ddagger}_{obsd}$ by use of relation (22),

$$H_{12} = H_{12}^{\circ}\{1 + (H^{\ddagger}/H_{12}^{\circ} - 1)\exp[-(2(r - r^{\ddagger})/(r_0 - r^{\ddagger}))^2]\} \tag{22}$$

where H_{12}° is H_{12} of eq 10 and $H_{12}^{\ddagger}$ is defined in eq 23, which uses an arbitrary continuous function to guarantee the correct behavior of the ground state in both the transition state and equilibrium regions.

$$H_{12}^{\ddagger} = E_2^s(r^{\ddagger}) - E_-^s(r_0) + \Delta G^{\ddagger}_{obsd} \tag{23}$$

We now obtain the Hamiltonian for the reaction in the enzyme active site by replacing the solvation energies of the ionic configurations by the electrostatic interactions with the enzyme active site. For example, in order to evaluate the potential surface for the above ionic bond cleavage in an enzyme active site, it is only necessary to replace $G_{sol}^{(i)}$ in E_i by the electrostatic interaction between the enzyme and the reacting species (referred to here as the "solvation" energy by the enzyme). This procedure is formally correct since we deal with identical substrates and the only difference is in their interaction with the medium (which is solution in one case and enzyme in the other).

III. Results

1. Potential Surfaces for Proton-Transfer Reactions. Many classes of chemical and biological processes involve proton-transfer reactions from an acid, A, to a base, B:

$$AH + B \rightarrow A^- + BH^+ \tag{24}$$

This section illustrates the evaluation of the potential surface for such a reaction: proton transfer to the glycoside oxygen of a sugar dimer R–O–R′. We describe below the construction and calibration of the solution potential surface and outline the comparison of the solution reaction with that in the enzyme active site.

(a) Valence Bond Potential Surface. The important resonance forms for this configuration are

$$\begin{aligned} \psi_1 &= (O_A\text{–}H\ O_B) \\ \psi_2 &= (O^-_A\ H^+\ O_B) \\ \psi_3 &= (O^-_A\ H\text{–}O^+_B) \end{aligned} \tag{25}$$

where O_A and O_B are the oxygen atoms of the acid donating the proton and the R–O–R′ molecule, respectively. These resonance forms were used in the study of the gas-phase hydrogen bond;[5] we use similar isolated molecule matrix elements with the modifications of Appendix 1. The solution Hamiltonian is obtained in the usual way by adding solvation terms to the diagonal matrix elements associated with ionic resonance forms (see Appendix 1). The ground-state potential surface is obtained from the lowest eigenvalue of this Hamiltonian; representative points on this surface are given in Table I. Although we will use solution

Table I. Calculations of Potential Surface for a Proton-Transfer Reaction in Solution[a]

geometry			total energy			configuration energy			ionic character		
r_1	r_2	r_3	$\bar{E}_G^s$	(E_G^s)	E_G^g	E_1^s	E_2^s	E_3^s	$(C_1^s)^2$	$(C_2^s)^2$	$(C_3^s)^2$
0.97	∞	∞	−108	−108[b]	−101	−74	196	3	0.92	0.09	0.00
0.97	2.70	1.73	−108	−108	−107	−70	204	−8	0.65	0.12	0.24
1.17	2.70	1.53	−106	−106	−98	−60	117	−20	0.38	0.15	0.46
1.37	2.70	1.33	−102	−102	−83	−49	68	−49	0.16	0.09	0.74
1.57	2.70	1.13	−97	−98	−79	−27	108	−70	0.09	0.09	0.82
1.77	2.70	0.93	−95	−97	−75	−13	68	−75	0.02	0.09	0.82
1.73	2.70	0.97	−97	−100	−78	−16	81	−79	0.02	0.09	0.82
2.73	3.70	0.97	−96	−99	−39	2	48	−78	0.02	0.10	0.88
3.73	4.70	0.97	−96	−99	−19	5	45	−78	0.02	0.10	0.88
4.73	5.70	0.97	−96	−99	−6	6	45	−78	0.02	0.10	0.88
∞	∞	0.97	−96	−99	1	6	47	−78	0.00	0.12	0.88

[a] Energies are in kcal/mol; r_1 and r_3 are the angstrom distances between the proton and O_A and O_B, respectively. r_2 is the O_A–O_B distance. E_G^s and $\bar{E}_G^s$ are, respectively, the calibrated and uncalibrated ground state energies for the reaction in solution. E_G^g is the ground-state energy in the gas phase; E_i^s is the energy of the indicated resonance forms in solution. C_i^s is the coefficient of the resonance forms in the eigenvector of the ground state of the reaction in solution. [b] The calculations of a solvated [AH + ROR'] system give, at $r_2 = \infty$, −104 kcal/mol rather than −108 kcal/mol, but this calculation does not include the charge-transfer interaction (H_{13}) between AH and the neighboring hydrogen-bonded water molecule. Thus, for $r_2 = \infty$ and $r_3 = \infty$ we perform the calculation for a solvated (AH- -OH_2 + R–O–R')system.

Table II. Calculations of Potential Surface for General-Acid Catalysis[a]

geometry			total energy			configuration energy				ionic character		
r_2	r_3	r_4	$\bar{E}_G^s$	(E_G^s)	E_G^g	E_1^s	E_3^s	E_4^s	E_5^s	$(C_3^s)^2$	$(C_4^s)^2$	$(C_5^s)^2$
2.7	1.73	1.48	−200	(−200)	−195	−137	−91	−47	35	0.10	0.15	0.00
2.7	1.73	2.0	−165	(−159)	−155	−107	−62	−80	−53	0.12	0.16	0.00
2.7	1.73	2.5	−156	(−149)	−125	−84	−38	−116	−79	0.01	0.80	0.03
2.7	1.73	3.0	−159	(−152)	−113	−75	−29	−121	−86	0.00	0.91	0.01
2.7	1.73	∞	−158	(−151)	−107	−70	−24	−120	−89	0.00	0.86	0.04
2.7	1.37	1.48	−194	(−194)	−170	−113	−45	−23	51	0.28	0.08	0.09
2.7	1.37	2.0	−167	(−156)	−131	−83	−89	−57	−80	0.28	0.12	0.16
2.7	1.37	2.5	−168	(−156)	−102	−60	−66	−92	−106	0.02	0.27	0.38
2.7	1.37	3.0	−173	(−161)	−91	−51	−50	−97	−113	0.01	0.27	0.36
2.7	1.37	3.5	−175	(−162)	−86	−48	−53	−97	−116	0.00	0.28	0.37
2.7	0.97	1.48	−190	(−180)	−128	−83	−146	7	−19	0.60	0.01	0.11
2.7	0.97	2.0	−172	(−160)	−109	−53	−116	−26	−108	0.42	0.01	0.36
2.7	0.97	2.5	−175	(−164)	−105	−30	−93	−18	−133	0.03	0.01	0.80
2.7	0.97	3.0	−178	(−169)	−99	−21	−84	−3	−140	0.01	0.01	0.82
2.7	0.97	∞	−181	(−171)	−78	−16	−79	100	−143	0.01	0.01	0.83
∞	0.97	1.98	−189	(−187)	−84	−61	−144	28	−23	0.85	0.00	0.14
∞	0.97	2.0	−172	(−160)	−44	−31	−114	−5	−112	0.42	0.00	0.43
∞	0.97	2.5	−176	(−166)	−18	−8	−91	3	−137	0.01	0.00	0.80
∞	0.97	3.0	−179	(−173)	−24	1	−82	18	−144	0.01	0.00	0.83
∞	0.97	∞	−182	(−175)	−25	6	−77	122	−147	0.00	0.00	0.83

[a] Notation as in Table I. r_4 is the C–O distance.

experiments to calibrate this surface, the ionic character of the transition state will not change significantly. It is important to note that the *uncalibrated* potential surface gives a proton-transfer energy for $r_2 = \infty$ of 9 kcal/mol, in good agreement with the experimental estimate of 12 kcal/mol of Appendix 2. Calculated enthalpies for proton transfer from H_2O to H_2O, from CH_3OH to H_2O and from HCOOH to H_2O, considered previously,[13] were within 5 kcal/mol of their observed values. Before comparing the solution and enzyme potential surfaces, we wish to start with the most accurate solution values we can; we therefore calibrate the matrix elements better to reproduce the experimental free energy of proton transfer.

(b) Calibration of the Solution Potential Surface Having obtained the approximate form of the ground-state potential surface, we now use the experimental estimate of ΔG_{PT}^S (Appendix 2) for calibration of the solution potential surface.

This is done by adjusting $\Delta^{(3)}$ in E_3^s to equalize the calculated and observed ΔG_{PT}^S, thus forcing the potential surface to have the correct value in the asymptotic region.

The off-diagonal matrix elements need not be changed since the calculated $\Delta G^{\ddagger}$ is within the experimental estimate (Appendix 2). The calibrated potential surface is presented in Figures 2 and 3 and Table I. As seen from Figure 3 and the table, the transition state possesses more than 50% ionic character. This indicates that electrostatic stabilization of the transition states in both the solution and enzymic reactions potentially has a very large effect on the activation energy.

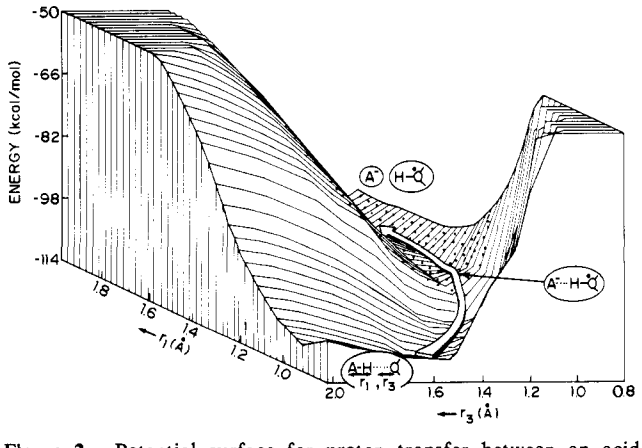

Figure 2. Potential surface for proton transfer between an acid $R''COO_AH$ and an RO_BR' molecule in solution. The independent coordinates r_1 and r_3 are respectively the distance from the proton to O_A and the $O_B\cdots O$ distance. The calculations are described in the text and in Table I. Regions of the potential surface that have more than 50% ionic character are dotted.

Table III. Experimental Determination of the Energies (in kcal/mol) at the Asymptotic Points of the Potential Surface of the General-Acid Catalysis Reaction[a]

configuration	notation	expression used	ΔG	ΔH^{gas}
$A^- + RO^+HR'$	ΔG_3^∞	$2.3RT[pK_a(AH) - pK_a(RO^+HR')]$	12 ± 2^b	147 ± 5^f
$A^- + R^+ + R'OH$	ΔG_4^∞	$\Delta G_3 + \Delta G_2$	26 ± 5^c	167 ± 5^f
$AH + R^+ + R'O$	ΔG_5^∞	$\Delta G_4^\infty + 2.3RT[pK_a(R'OH) - pK_a(AH)]$	41 ± 5^d	215 ± 5^f
$A^- + R^+ \cdots OHR'$	$\Delta G_{3,5}^\ddagger$	$\Delta G_3^\infty + \Delta G_2^\ddagger$	29 ± 2^e	

[a] ΔG_i is given relative to G_1 at the equilibrium configuration of AH + R-O-R'. The superscript ∞ indicates that fragments are at infinite separation. [b] Using $pK_a(AH) = 4$ and $pK_a(ROHR') = -5$.[24] [c] Using ΔH^{gas} of this table and the calculated ΔG_{sol}. [d] Using $pK_a(ROH) = 15$.[20] [e] Using $\Delta G_2^\ddagger = 18$ kcal/mol; see discussion in Appendix 2. [f] From Table VI.

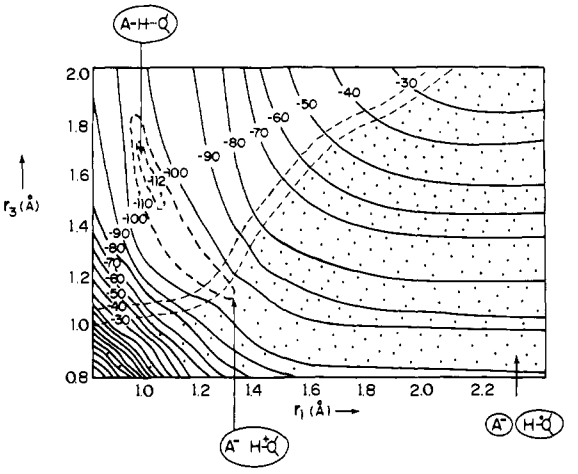

Figure 3. The change in ionic character in the potential surface of the proton-transfer reaction. A contour representation of the potential surface of Figure 2 with emphasis on the change in ionic character during the reaction. The lines divide regions with greater than 50% ionic character (dotted) from those with less than 50% ionic character.

(c) Using the Solution Potential Surface in Studying Enzymic Reactions. The potential surface obtained above is only a rough approximation, but it can serve as a basis for comparison with the potential surface and activation energy in enzyme catalysis. This is accomplished by replacing $G_{sol}^{(i)}$ in the diagonal matrix elements by the electrostatic interaction with the enzyme, $V_{Qq}^{(i)} + V_{Q\alpha}^{(i)}$ (see eq 19 and 20). The comparison of proton transfer in aqueous solution with that in the active site of lysozyme is illustrated in Figure 7; the detailed calculations will be presented in a subsequent paper.

2. Potential Surface for a General-Acid Catalysis Reaction. General-acid catalysis reactions are among the most extensively studied in physical organic chemistry,[1,14-16] but the potential surface for such a reaction in solution has not yet been described quantitatively. In this section we will demonstrate the construction of such a potential surface for hydrolysis of a disaccharide.

We consider the following steps in the acid-catalyzed hydrolysis of a disaccharide:

$$ROR' + AH \rightleftharpoons ROH^+R' + A^- \rightleftharpoons R^+ + A^- + R'OH \quad (26)$$

Analysis of experimental information about such a reaction is described in Appendix 2 and is based largely on information from the so-called "specific-acid catalysis" reaction, where the acid is an H_3O^+ ion. The relation between the free energies of specific-acid catalysis and general-acid catalysis is outlined in Figure 4 and explained in detail in Appendix 2. In this section, we will describe the construction of the EVB potential surface, its calibration and the use of the calibrated surface in comparing general-acid catalysis in solution and in the active site of lysozyme.

(a) Valence Bond Hamiltonian. In order to obtain a quantitative estimate of the potential surface of the general acid catalysis reaction, we consider the resonance forms in eq 27. The Hamiltonian for these resonance forms is evaluated by the scheme of section II. The functions used are given in Appendix 1.

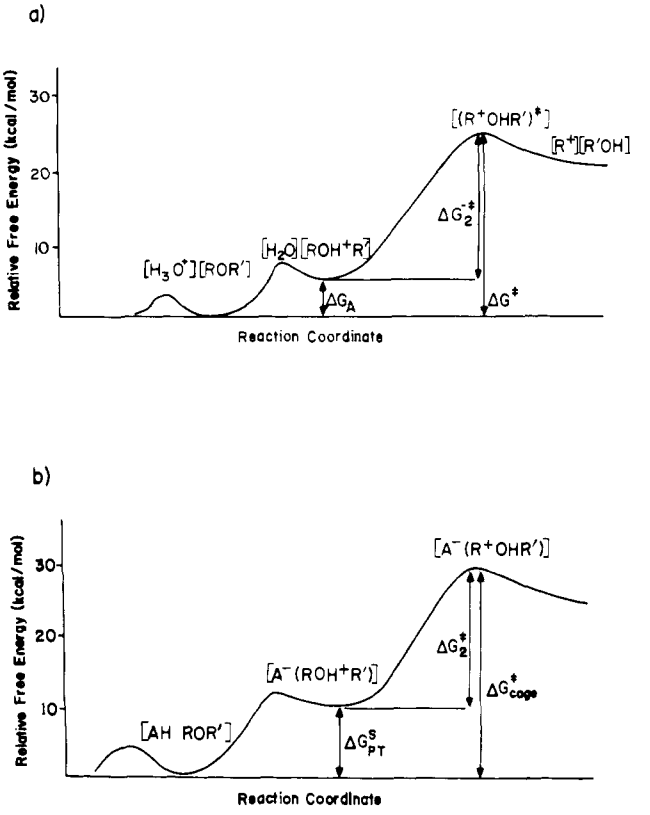

Figure 4. Analysis of the energetics of (a) specific-acid catalysis and (b) general-acid catalysis. As discussed in the text, ΔG_A is the free energy of proton transfer from H_3O^+ to ROR', $\Delta \bar{G}_2^\ddagger$ is the activation free energy of cleavage of the protonated C–O bond, ΔG_{PT}^S is the free energy for proton transfer from AH to ROR', $\Delta G_2^\ddagger$ is the activation free energy of cleavage of the protonated C–O bond in the presence of A^- in the same solvent cage and $\Delta G^\ddagger_{cage}$ is the activation free energy for general-acid catalysis when AH and ROR' are in the same solvent cage.

$$\psi_1 = (A\text{-}H\ R\text{-}OR') \qquad \psi_4 = (A\text{-}H\ R^+\ {}^-OR')$$
$$\psi_2 = (A^-\ H^+\ R\text{-}OR') \qquad \psi_5 = (A^-\ R^+\ H\text{-}OR') \quad (27)$$
$$\psi_3 = (A^-\ R\text{-}OH^+R') \qquad \psi_6 = (A^-\ H^+\ R^+\ {}^-OR')$$

(b) Calibration of the Solution Potential Surface. As before, we calibrate the solution potential surface in asymptotic regions by using the experimental results summarized in Table III, adjusting $\Delta^{(i)}$ in E_i to fit the calculated and observed $\Delta G^{(i)}$ of reaction for $i = 3$–5. Further calibration of the surface is obtained by considering the potential surface for breaking the protonated C–O bond in specific-acid catalysis. This involves the resonance forms ψ_3 and ψ_5 with A^- at infinite distance. Using the observed activation free energy, $\Delta \bar{G}_2^\ddagger$, for this reaction (see Appendix 2) we calibrate H_{53} by means of eq 23 where

$$H_{53}^\ddagger = [E_3^s(\mathbf{r}^\ddagger) - E_3^s(\mathbf{r}_0)] - \Delta \bar{G}_2^\ddagger \quad (28)$$

The resulting potential surface for dissociation of the protonated bond is illustrated in Figure 5. The calibrated matrix elements give the potential surface shown in Figure 6.

(14) Capon, B. *Chem. Rev.* **1969**, *69*, 407–498.
(15) Dunn, B. M.; Bruice, T. C. *Adv. Enzymol. Relat. Areas Mol. Biol.*, **1973**, *37*, 1–59.
(16) Fife, T. H. *Adv. Phys. Org. Chem.* **1975**, *11*, 1–122.

Table IV. Comparison of General-Acid Catalysis in Solution and in Lysozyme[a]

system	water cage			enzyme				
	ΔG^{gas}	ΔG_{sol}	ΔG_{tot}	ΔG^{gas}	$\Delta V_{Q\alpha}$	$\Delta V_{Q\alpha}$	ΔG_{sol}^{P}	ΔG_{tot}
$(A^- ROH^+ R)$	57	−47	$\Delta G_{PT}^{cage} - 10$	57	−15	−40	−55	$\Delta G_{PT} \simeq 3$
$(A^- \cdots R^+ \cdots OHR)$	78	−46	$\Delta G^{\ddagger}_{cage} \simeq 28$	$78 + 5^b$	−17	−44	−63	$\Delta G^{\ddagger}_{cat} \simeq 19$

[a] All energies are given in kcal/mol. ΔG^{gas} is the gas-phase free energy for formation of the indicated systems from the equilibrium [AH ··· ROR] system. This value is obtained from the calibrated EVB potential surface with an estimated contribution of −5 kcal/mol for the entropy associated with the motion of the fragments of the $R^+ \cdots OHR$ system in $[A^- \cdots R^+ \cdots OHR]$. ΔG_{sol} is the calculated solvation energy of the ground-state charge distribution of the indicated system. The calculations simulated Glu 35 by a formic acid and the substrate by a disaccharide. $\Delta G_{Q\alpha}$ and ΔV_{Qq} are, respectively, the changes in inductive interactions and charge-charge interactions (relative to [AH ··· R-O-R]) between the indicated system and the enzyme active site that includes the ionized Asp 52. ΔG_{sol}^{P} is the sum of $\Delta V_{Q\alpha}$ and ΔV_{Qq}. ΔG_{tot} is the calculated energy of the EVB ground state, which is given to a good approximation by $\Delta G^{gas} + \Delta G_{sol}$. [b] ΔG^{gas} in the water cage includes an estimate of −5 kcal/mol due to motion of the $[R^+ \cdots OHR]$ fragments; this contribution is not included in ΔG^{gas} in the enzyme case where the motion of the fragments is restricted.[10]

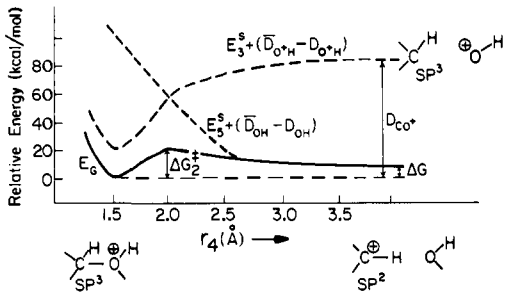

Figure 5. The potential surface for the $ROH^+R' \rightarrow R^+ + HOR'$ reaction. E_G is the ground-state energy; E_3^s and E_5^s are the energies of the corresponding configurations in eq 27. The additions of the D–$\bar{D}$ terms correspond to stabilization by interaction with ψ_6. r_4 is the C–O distance. The figure indicates the stable hybridization of the carbon in the three limiting cases. The "experimental" estimate of $\Delta\bar{G}_2^{\ddagger}$ is used to calibrate the potential surface for the general-acid catalysis reaction.

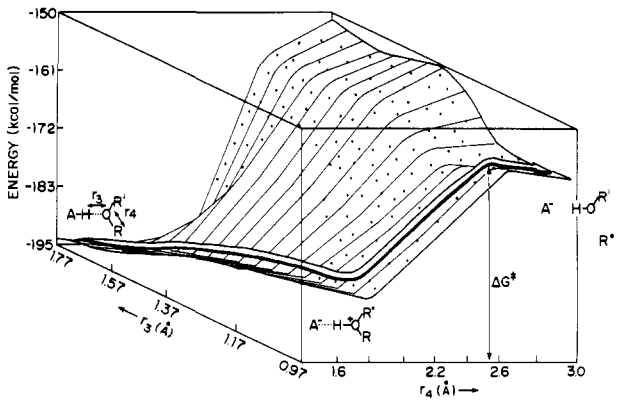

Figure 6. Potential surface for a general-acid catalysis reaction in solution. The calculations are described in the text and in Table II. r_3 and r_4 are the O_B–H and C–O distances, respectively. Regions of the potential surface with more than 50% ionic character are dotted.

(c) Potential Surfaces for Enzymic Reactions. The use of the calibrated potential surface in studying enzymic reactions will be demonstrated here by considering the catalytic reaction of lysozyme.[18,12] This reaction (Figure 7) involves proton transfer from glutamic acid 35 (Glu 35) to O_4 of the polysaccharide, cleavage of the protonated $C-O_4$ bond and stabilization of the carbonium ion transition state by the ionized aspartic 52 (Asp 52).

The rate k_{cat} of general-acid catalysis by lysozyme is $\sim 1\ s^{-1}$ at pH 5.25.[17] This corresponds to an activation free energy, $\Delta G^{\ddagger}_{cat}$, of ~18 kcal/mol. The activation free energy $\Delta G^{\ddagger}_{cage}$ of the reference reaction in the water cage is 26 ± 2 kcal/mol according to the estimate of Appendix 2. In order to understand the origin of the difference between $\Delta G^{\ddagger}_{cat}$ in the enzyme and $\Delta G^{\ddagger}_{cage}$ of the reference reaction in a solvent cage, we performed the calculations summarized in Figure 7 and Table IV. We

Table V. Parameters Used in Evaluating the Hamiltonian Matrix Elements

(1) Morse Potential

bond	$\bar{D}$[a]	D	a[d]	b_0[e]
O-H	75	102[b]	2.35	0.96
O^+-H	75	97[c]	2.35	0.96
C-O	67	92[b]	2.06	1.43
C-O^+	67	76[c]	2.06	1.43

(2) Gas-Phase Energies of Ionic States[f]

fragment	Δ	value, kcal/mol
$HCOO^- + H^+$	I − EA	240
$R'O^- + H^+$	I − EA	272
$R'O^- + R^+$	I − EA	120
$HCOO^- + ROH^+R'$	$\Delta^{(3)}$	140
$HCOO^- + R^+ + R'OH$	$\Delta^{(5)}$	77

(3) Nonbonded Potential Functions[g]

atom	b	$\bar{a}$	r^*	ϵ^*
H^+O^-	3470	2.5		
C^+O^-	5288	2.5		
H^+O	1500	2.5		
HO^-	65	2.5		
HO	65	2.5		
OO^-			3.56	0.085

[a] The $\bar{D}$ are evaluated by using eq 8 with the values 105, 51, and 88 kcal/mol for $\bar{D}_{HH}$, $\bar{D}_{OO}$, and $\bar{D}_{CC}$, taken from bond dissociation energies in H_2, H-O-O-H and C_2H_6.[22] It is assumed, following ref 5, that $\bar{D}_{O^+Y} = \bar{D}_{OY}$.[b] Taken from ref 22. [c] From Table VI. [d] Using force constants from ref 23 and the D of the present work. [e] From ref 2. [f] Evaluated by using the experimental information given in Table VI and the expressions for the corresponding energies in eq 9, 29, and 34. [g] The nonbonded interactions of H^+O^-, C^+O^-, H^+O, HO^-, and HO are represented by $V_{nb} = b \exp\{-\bar{a}r\}$. The parameter $\bar{a}$ is taken as 2.5 for H^+O^-;[6] the same value is chosen for all other interactions since the correlation between b and a is too large to determine them independently. The value of b for H^+O^- and O^-C^+ was determined by requiring that the minimum of $(V_{nb} - e^2/r)$ be at the sum of the corresponding univalent ionic radii (the univalent radii are taken from ref 2). The values of b for H^+O and HO were determined by fitting the calculated and observed gas-phase equilibrium distances and dissociation energies of the water dimer. The OO^- nonbonded interaction is represented by 12-6 potential functions where the parameter ϵ^* is taken from ref 12 and r^* was obtained by fitting the calculated and observed geometry and dissociation energy of the gas-phase water dimer.

replaced the solvation energy contributions $G_{sol}^{(i)}$ in the calibrated potential surfaces of the substrate + glutamic acid (S + Glu) system in aqueous solution by the electrostatic interaction between the (S + Glu) system and the rest of the enzyme, including Asp 52.

The calculated difference between the activation energies $\Delta G^{\ddagger}_{cage}$ and $\Delta G^{\ddagger}_{cat}$ (Figure 7 and Table IV) is about 7 kcal/mol, in good agreement with the corresponding experimental estimate (~8 kcal/mol). Similar agreement was obtained in a previous work[10] which compared the stabilization of the ψ_5 ionic config-

(17) Chipman, D. M. *Biochemistry* **1971**, *10*, 1714–1722.
(18) Philips, D. C. *Sci. Am.* **1966**, *215* (5), 78–90.

Table VI. Gas-Phase Enthalpies Used to Determine the Energies of the Ionic States

entry	process	expression used	ΔH, kcal/mol
1	$R'OR \rightarrow R'O^- + R^+$	$D + I - EA$	215[a]
2	$R'OH \rightarrow R'O^- + H^+$	$D + I - EA$	376[b]
3	$HCOOH \rightarrow HCOO^- + H^+$	$D + I - EA$	345[c]
4	$HCOOH + H_2O \rightarrow HCOO^- + H_3O^+$	$\Delta H_{PT}{}^g$	177[d]
5	$CH_3OH + H_2O \rightarrow CH_3O^- + H_3O^+$	$\Delta H_{PT}{}^g$	211[d]
6	$HCOO^- + R'OH \rightarrow HCOOH + R'O^-$	$\Delta H_{PT}{}^g$	44[e]
7	$HCOOH + ROR' \rightarrow HCOO^- + ROH^+R'$	$\Delta H_{PT}{}^g$	147[f]
8	$HCOOH + ROR' \rightarrow HCOO^- + R^+ + R'O$	$\Delta H_{PT}{}^g$	167[g]
9	$ROH^+R' \rightarrow R^+ + R'OH$	ΔH	20[h]
10	$ROH^+R' \rightarrow R\cdot + R'OH^+$	$\Delta H + I_{R\cdot} - I_{R\cdot OH}$	76[i]
11	$ROH^+R' \rightarrow RO^+R' + H\cdot$	$PA_{ROR'} - I_H + I_{ROR'}$	97[j]

[a] Taking $I_{i\text{-}C_3H_7} = 180$ kcal/mol,[24] $EA(C_2H_5O\cdot) = 40$ kcal/mol,[25] $D_{CO} = 91$ kcal/mol[22] gives $\Delta H = 230$ kcal/mol for $i\text{-}C_3H_7\text{-}O\text{-}C_2H_5$. This gives $\Delta H = 215 \pm 5$ kcal/mol by interpolating EA and I to the corresponding values where R and R' are sugar residues. This is done by using the trend of change of I and EA with the size of R.[24-26] [b] Reference 25. [c] Reference 27. [d] References 27 and 28. [e] From the differences between $\Delta H_{PT}{}^g$ in entries 4 and 5. [f] From the difference between ΔH in entry 3 and the proton affinity of R–O–R', which is estimated here as 198 ± 5 kcal/mol from the trend in related compounds in ref 26 and 28. [g] From $\Delta H_{PT}{}^g$ of entry 7 and ΔH of entry 9. [h] The estimate of $\Delta H = 20 \pm 5$ kcal/mol is based on related reactions in ref 29. [i] ΔH is taken from entry 9 and $I_{R\cdot}$ is taken from footnote *a* in this table. $I_{R'OH}$ is evaluated by taking $I_{CH_3CH_2OH} = 241$ kcal/mol[26] and estimating the inductive effect of replacing CH_3CH_2 by R' (using the trend in ref 26). This gives $I_{R'OH} = 236 \pm 5$ kcal/mol. [j] The proton affinity, PA, of ROR is taken as 195 kcal/mol from footnote *f* of this table, $I_H = 312$ kcal/mol[22] and $I_{ROR'} = 214 \pm 5$ kcal/mol by taking I of diethyl ether from ref 27 as 219 kcal/mol and estimating the effect of replacing CH_3CH_2 by R.

uration in solution and in the enzyme active site. Considering only ψ_5 turns out to be a reasonable approximation since, as illustrated in Table II, this configuration is the most important one ($c_5 = 0.8$) in the transition-state region.

The main point that emerges from the present calculations and from the simpler calculations of ref 10 is that electrostatic interactions between the enzyme active site and the ionic resonance forms of the reacting system can account quantitatively for the rate enhancement by the enzyme. The agreement between the calculated and observed differences in activation energies of the reaction in solution and in enzyme indicates that the EVB method is a promising approach for correlating the structures of enzymes with their catalytic activities.

IV. Concluding Remarks

This paper presents an empirical valence bond (EVB) approach that allows one to obtain approximate potential surfaces for reactions in solution. The approach relies on the simple valence bond concepts of ionic–covalent resonance to obtain the Hamiltonian of the isolated system and then obtains the solution Hamiltonian by adding solvation energies to the diagonal matrix elements. The method allows for very convenient calibration of the Hamiltonian matrix elements by comparing them to observed pK_a values and other experimental information about solution reactions. Use of the EVB approach provides a simple and reliable estimate of the ionic character of transition states in different environments. Such an estimate is of crucial importance in studying enzymic reactions.[10]

The main purpose of the EVB approach is not to give a recipe for obtaining potential surfaces of reactions in solution but to provide a reliable tool for *comparing* enzymic reactions with

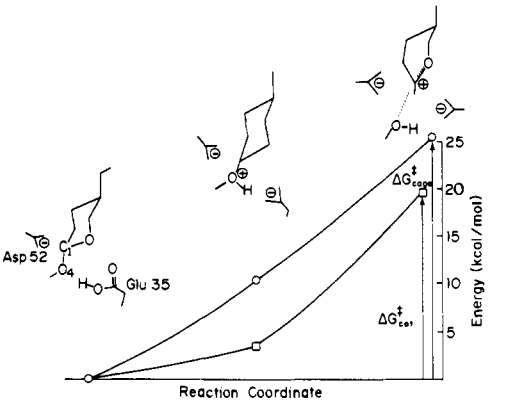

Figure 7. Comparison of general-acid catalysis in aqueous and enzyme environments. The figure presents the calculated potential surfaces for hydrolysis of the C_1–O_4 glysocidic bond in an aqueous solvent cage (○) and in the active site of lysozyme (□). The activation energies $\Delta G^{\ddagger}_{cage}$ and $\Delta G^{\ddagger}_{cat}$ are evaluated as described in the text.

solution reactions. This can be done (as is demonstrated in ref 10) by taking the calibrated solution potential surface and replacing the solvation energies of the ionic configurations by the corresponding electrostatic interactions with the enzyme.

Acknowledgment. This work was supported by Grant GM 24492 from the National Institute of Health and by the Alfred P. Sloan Foundation. Part of the work was done at a CECAM workshop in Orsay during summer 1979.

Appendix 1. Determination of EVB Matrix Elements

This appendix describes in detail determination of the EVB Hamiltonian matrix elements for proton transfer and general-acid catalysis.

(a) EVB Hamiltonian for Proton-Transfer Reactions. Proton-transfer reactions involve the three resonance forms given in eq 25. These resonance forms have been used in the study of the gas-phase hydrogen bond.[5] The energies of these resonance forms are determined by the approach of section II as

$$E_1{}^s = \bar{M}_{OH}(r_1) + V_{nb}{}^{(1)}$$

$$E_2{}^s = \Delta^{(2)} + V_{QQ}{}^{(2)} + V_{nb}{}^{(2)} + G_{sol}{}^{(2)} + V_{ind}{}^{(2)}(r_3) \quad (29)$$

$$E_3{}^s = \bar{M}_{OH^+}(r_3) + \Delta^{(3)} + V_{QQ}{}^{(3)} + V_{nb}{}^{(3)} + G_{sol}{}^{(3)}$$

where r_1 and r_3 are the distances between the hydrogen and O_A and O_B, respectively. The $\bar{M}_{XY}$ is the covalent Morse potential for the indicated bonds and $\Delta^{(2)}$ and $\Delta^{(3)}$ are given by $\Delta^{(2)} = I_H - EA_O$ and $\Delta^{(3)} = \Delta H_{PT}{}^g + (D_{O^+H} - D_{OH})$, where $\Delta H_{PT}{}^g$ is the gas-phase energy for proton transfer from A to R–O–R' at infinite separation. $V_{QQ}{}^{(i)}$ is the electrostatic interaction between the charged fragments in the ith configuration, where the atomic charges $Q_\mu{}^{(i)}$ of each fragment in the ith configuration are evaluated quantum mechanically for the isolated fragments (here we use the MINDO/2 charges[19]). V_{nb} is the nonbonded interaction between the fragments (excluding $V_{QQ}{}^{(i)}$). The potential functions used for V_{nb} are given in Table V. $G_{sol}{}^{(i)}$ is the solvation free energy of the ith configuration. $V_{ind}{}^{(2)}$ is the inductive interaction between the positive charge on the hydrogen and the induced dipoles of the oxygen electrons; this is given (in kcal/mol) by $V_{ind}{}^{(2)} = -166\alpha_O/r^4$ where α_O is the atomic polarizability of oxygen (0.8 Å^3). A more rigorous treatment would include other charge-induced dipole interactions in the diagonal matrix elements.

All the parameters used in evaluation of the above expressions are listed and discussed in Table V.

The off-diagonal elements that represent the interactions between resonance forms are evaluated as follows: H_{12} and H_{23} are determined by equation 11 as

$$H_{12} = L_{12}(r_1) \qquad H_{23} = L_{23}(r_3) \quad (30)$$

H_{13} is not assumed to be zero (as it would be in the procedure

(19) Dewar, M. J. S.; Haselbach, E. *J. Am. Chem. Soc.* **1970**, *92*, 590–598.

of section II) but is determined by the approach of ref 5 (assuming all $|S_{OH}|^2 \ll 1$) as

$$H_{13} = S_{O_BH} H_{12} \tag{31}$$

where O_B is the oxygen of the R–O-R′ molecule (see eq 25) and S_{O_BH} is the overlap integral between the 1s orbital of the hydrogen atom and the 2p orbital of O_B. These integrals are evaluated analytically by using the Slater orbitals.

(b) EVB Hamiltonian for General-Acid Catalysis Reactions. The Hamiltonian involves the six resonance forms of eq 27; the first three are those evaluated above for proton transfer; their energies are expressed now as

$$\begin{aligned} E_1^s &= (E_1^s)^{PT} + \bar{M}_{CO} \\ E_2^s &= (E_2^s)^{PT} + \bar{M}_{CO} \\ E_2^s &= (E_3^s)^{PT} + \bar{M}_{CO} \end{aligned} \tag{32}$$

where $(E_i^s)^{PT}$ is the ith diagonal element from eq 29. $\bar{M}_{CO}$ is the covalent Morse potential for the C–O bond. The off-diagonal elements H_{12}, H_{13}, and H_{23} are evaluated as in the proton-transfer (PT) reaction (eq 30 and 31).

$$H_{12} = H_{12}^{PT} \qquad H_{13} = H_{13}^{PT} \qquad H_{23} = H_{23}^{PT} \tag{33}$$

The energies of the other resonance forms evaluated by the approach of section II are

$$\begin{aligned} E_4^s &= \bar{M}_{OH}(r_1) + \Delta^{(4)} + V_{QQ}^{(4)} + G_{sol}^{(4)} \\ E_5^s &= \Delta^{(5)} + V_{QQ}^{(5)} + \bar{M}_{OH}(r_3) + V_{nb}^{(5)} + G_{sol}^{(5)} \\ E_6^s &= \Delta^{(6)} + V_{QQ}^{(6)} + V_{nb}^{(6)} + V_{ind}^{(6)}(r_2) + G_{sol}^{(6)} \end{aligned} \tag{34}$$

where $\Delta^{(4)} = I_R - EA_{RO}$, $\Delta^{(5)} = \Delta^{(4)} + \Delta H_{PT}^g(AH + R'O^- \rightarrow A^- + R'OH)$ (Table VI) and $\Delta^{(6)} = \Delta^{(2)} + \Delta^{(4)}$. The other terms in these equations are as previously described.

The off-diagonal elements that are not included in eq 34 are evaluated by the approach of section II. That is, whenever the resonance forms i and j differ only by the presence of a bond (e.g., the difference between ψ_2 and ψ_6 is the R–O bond), H_{ij} is given by $L_{ij}(r_l)$.

$$\begin{aligned} H_{14} = L_{14}(r_4) \qquad H_{35} = H_{14} \qquad H_{26} = L_{26}(r_4) \\ H_{46} = L_{46}(r_1) \qquad H_{56} = L_{56}(r_3) \end{aligned} \tag{35}$$

This forces bond energy dependence on r_l of the ith resonance form to reproduce the observed Morse potential. All other off-diagonal elements are zero according to the rules given in ref 4 and are proportional to S^2 and S^3 in the approximation given in ref 5. These elements are set here to zero.

Appendix 2. Experimental Analysis for Calibration of EVB Potential Surfaces

(a) Experimental Analysis of the Energies of the Proton-Transfer Reaction. The free energy of proton transfer in solution from AH to R–O–R′ at infinite separation is given by eq 36. With estimates of $pK_a \simeq 4$ for a carboxylic acid in solution and $pK_a = -5 \pm 1$ for the protonated oxygen,[20] we obtain, $\Delta G_{PT}^S \simeq 12$ kcal/mol at 300 K.

$$\Delta G_{PT}^S = 2.3RT[pK_a(AH) - pK_a(ROH^+R')] \tag{36}$$

It is known from experiments in solution[11] that the rates of ion recombination reactions are diffusion controlled (activation energy ≤ 5 kcal/mol). Thus, the total activation energy of the reaction is bounded by eq 37. These estimates of ΔG_{PT}^S and $\Delta G^\ddagger$ can be used to calibrate the potential surface for the solution reaction.

$$\Delta G^\ddagger < \Delta G_{PT}^S + 5 \tag{37}$$

(b) Experimental Analysis of the General-Acid Catalysis Reaction. Acid-catalyzed reactions include steps in eq 38, where

$$ROR' + AH \underset{k_{-1}}{\overset{k_1}{\rightleftharpoons}} ROH^+R' + A^- \overset{k_2}{\rightleftharpoons} R^+ + A^- R'OH \tag{38}$$

in our case R and R′ are sugar residues. We analyze here some of the experimental information about such reactions[14-16] in terms of free energies. Most of the experimental information is related to the so-called "specific-acid catalysis" reaction (eq 39), where the acid is a hydronium ion. The observed rate for this reaction is given approximately[15] by eq 40, where K_a is the acid-dissociation constant of the protonated reactant.

$$ROR' + H_3O^+ \underset{k_{-1}}{\overset{k_1}{\rightleftharpoons}} ROH^+R' + H_2O \overset{k_2}{\rightleftharpoons} R^+ + R'OH + H_2O \tag{39}$$

$$k_{obsd} \simeq k_2(k_1/k_{-1})[H_3O^+]/[H_2O] = k_2/(K_a[H_2O])[H_3O^+] = k'_{obsd}[H_3O^+] \tag{40}$$

$$K_a = [H^+][ROR']/[ROH^+R'] \tag{41}$$

For a typical glycoside hydrolysis $k_{obsd} \simeq 10^{-4}$ at 0.1 M H^+ and a temperature of 70 °C. With a typical[24] K_a of 10^{-4}–10^{-6} M we obtain from eq 40 $k_2 = 1$–100 s^{-1}. By absolute rate theory we have

$$\begin{aligned} k_2 &= (k_BT/h)\exp\{-\Delta\bar{G}_2^\ddagger/RT\} \\ k'_{obsd} &= (k_BT/h)\exp\{-\Delta G^\ddagger_{obsd}/RT\} \end{aligned} \tag{42}$$

for the processes illustrated in Figure 3a. This gives $\Delta\bar{G}_2 = 17$–18 kcal/mol and $\Delta G_{obsd} = 23$–24 kcal/mol. With these estimates the activation free energy of the reaction can be written as

$$\Delta G^\ddagger_{obsd} = \Delta G_A + \Delta\bar{G}_2^\ddagger \tag{43}$$

where $\Delta G_A = -RT \ln (K_a[H_2O])$ is the free energy for proton transfer from H_3O^+ to R–O–R′ taking the standard state as one molar concentration. These considerations are summarized in Figure 3a.

When the H_3O^+ catalyst is replaced by an acid AH, the reaction is an example of general-acid catalysis. The kinetics of this type of reaction is complicated by the competing acidic activity of H^+. However, the activation energy for the general-acid catalysis reaction, which occurs when AH and R–O–R′ are in the same solvent cage, can be estimated by using information from the specific-acid catalysis reaction. This is done, as demonstrated in Figure 3b, by considering two steps: (i) proton transfer from A to R–O–R′ with free energy ΔG_{PT}^S; (ii) hydrolysis of the protonated sugar in the presence of A^-, with free energy $\Delta G_2^\ddagger$. The overall activation free energy is given by eq 44, where ΔG_{PT}^S is

$$\Delta G^\ddagger_{cage} = \Delta G_{PT}^S + \Delta G_2^\ddagger \tag{44}$$

the free energy for proton transfer from AH to the sugar at infinite separation given by eq 36. The present calculations indicate that $\Delta G_2^\ddagger$ is given to a good approximation by $\Delta\bar{G}_2^\ddagger$ of the previously analyzed specific-acid catalysis reaction, the activation free energy for dissociation of the protonated R–O bond. The value of $\Delta G^\ddagger_{cage}$ determines the rate constant k_{cage} for general-acid catalysis of R–O–R′ by an acid locked with it in the same solvent cage. Estimating the actual contribution of general-acid catalysis to the observed rate requires careful consideration of the competing reaction catalyzed by H_3O^+, the possibility of donation of the AH proton to the bulk water and the probability that AH and the sugar are in the same cage. However, our k_{cage} is still the upper limit for the rate of catalysis by AH. Thus, despite the fact that analysis of the kinetics of general-acid catalysis is complicated, the estimate of the activation free energy for general-acid catalysis in a solvent cage is simple. The experimental estimates of the free energies at asymptotic points of the potential surface for general-acid catalysis are summarized in Table III.

(20) Arnett, E. M. *Prog. Phys. Org. Chem.* **1963**, *1*, 223–411.
(21) Bunton, C. A.; DeWolfe, R. H. *J. Org. Chem.* **1965**, *30*, 1371–1378.
(22) Benson, S. W. *J. Chem. Educ.* **1965**, *42*, 502–518.
(23) Wilson, E. B.; Decius, J. C.; Cross, P. C. "Molecular Vibrations"; McGraw-Hill Inc.: New York, 1955.
(24) Franklin, J. L.; Dillard, J. G.; Rosenstock, H. M.; Herron, J. T. *Natl. Stand. Ref. Data Ser. (U.S., Natl. Bur. Stand.)* **1969**, *NSRDS-NBS 26*.
(25) McIver, R. T.; Miller, J. S. *J. Am. Chem. Soc.* **1974**, *96*, 4323–4325.
(26) Beauchamp, J. L. *Annu. Rev. Phys. Chem.* **1971**, *22*, 527–561.
(27) Bartmess, J. E.; McIver, R. T. *Gas Phase Ion Chem.* **1979**, *2*.
(28) Kebarle, P. *Annu. Rev. Phys. Chem.* **1977**, *28*, 445–476.
(29) Hiraoka, K.; Kebarle, P. *J. Am. Chem. Soc.* **1977**, *99*, 360–366.